Red Shift Phenomena revealed in the Zonal Winds Oscillations Probably Induced by the Sunspot Cycle

Gyu-Ho Lim*

SEES, Seoul National University, Seoul 151-747, Korea

Ae-Sook Suh

KMA, Shindaebang-Dong 460-18, Seoul 156-720, Korea

Yongcheol Suh

Department of Civil Engineering, The University of Tokyo

4-6-1 Komaba, Meguroku, Tokyo 153-8505, Japan

Corresponding author address: Associate professor Gyu-Ho Lim, SEES, College of Natural Sciences, Seoul National University, Seoul 151-747, South Korea.
E-mail: gyuholim@snu.ac.kr

ABSTRACT

By inter-comparing exhaustively the results of wavelet analysis of the sunspot cycles and apparently associated oscillations in the time series of the zonal winds over the tropics, we found convincing evidences of the frequency shift of the oscillations, especially in the lower troposphere. The frequency of the oscillations forced by sunspot cycle decreased considerably in the lower troposphere, which is an analogue of the gravitational red shift or the doppler red shift even though their mechanisms are obviously different for each shift. The red shift revealed in our analysis may be

explained with the framework of a damped harmonic oscillator forced by the oscillatory forcing due to the variation of sunspot number in time. However, the forcing is not so strong or effective that it could not drive continuously the observed oscillations in the atmosphere. By examining the frequency change of a sinusoid which has been modulated in frequency, we showed a probable functioning of red shift in the time series of the sunspot-induced oscillations in the lower troposphere.

The implications of our finding of the ‘red shift’ phenomenon are fundamental for investigating and understanding of the atmospheric wave phenomena and their possible connections to the remote forcing and/or the induced motions in distant place of the atmosphere. The conventional analysis method using the coefficients of correlation or their sophisticated derivatives would be very sensitive to the data time period in investigating any connections between the oscillations manifesting frequency shift. The value of the correlations between the oscillations involved in frequency modulation will go to zero in general when increasing the data period for analysis, as evident from the coefficient of correlation between the two sinusoids with different periodicity.

1. Introduction

In the past until 18th century, the sunspot cycle was esteemed as an attractive indicator for the decadal prediction of the earth climate because of the well known about 11- year cyclic behavior of the sunspot numbers. In fact many authors sought relationships of the solar activity with the surface temperature, pressure, and precipitation as well as the annual crop yields. However, their conclusions were so controversy that in a certain case the same data sets gave the different results to different authors. Many ambiguous results in the past seem to force meteorology researchers to evade the topics these days. The explicit investigation of the topics was very rare in recent years when considering the number of related literatures in the period before Lanzante (1979), who gave a brief but reasonable exception against Hancock and Yarger's (1979) claim of connection of solar activity with weather.

In that period, Kim (1976) found some connections of the summer precipitation and winter temperature of the Korean Peninsula to sunspot cycle, especially stronger connection before year 1900. From the analysis of 60-year precipitation, pressure, temperature of the southern part of the Korean Peninsula, Moon and Moon (1981) claimed the sunspot cycle related periods in the time series of the above meteorological variables. The latest paper dealing with the topics is by van Loon and Labitzke (1998) in a great endeavor, following their previous works of Labitzke and van Loon (1993; 1995) and van Loon and Labitzke (1990; 1994). The methods of analysis employed by the previous authors were basically the same as the conventional methods such as the coefficients of correlation, the power spectrum analysis, and the composite analysis. A correlation or power spectrum analysis has been widely used with a great success for clarifying relations between the meteorological phenomena.

For identifying connections between the sunspots and meteorological phenomena, Shapiro (1975) examined the monthly mean temperatures by Manley (1974). In contrast with his exclamation of no relations between the sunspots and the temperatures, Bain (1975) and Dyer (1976) released their findings of 11-year cycle and a 22-year cycle from the same data. Hancock and Yarger (1979) supported the connection of the United States' weather to the sunspot cycle and the derived double cycle from the sunspot cycle. Gerety et al. (1977) conducted exhaustively cross-spectral analysis of the single and double sunspot cycles and temperature and precipitation of the contiguous United States. Based on their analysis of comprehensive volume of data for the globe, they negated the previous positive results even they left a room for any unknown processes that would connect sunspot cycle and weather. Hancock and Yarger (1978) attributed the above seemingly contradictory results solely due to the different analysis methods. However, the basic analysis methods utilized by various authors are virtually the same when considering their use of correlation and cross-spectrum analysis for their results.

Despite of the excellence of the correlation analysis in general for identifying connections between the oscillatory atmospheric motions, it has an intrinsic limitation for the oscillations having frequency shift. In this paper, the terms of 'frequency shift' will be used as denoting a reasonably small change of power distribution in the frequency or period domain as a function of time. Those oscillations with slightly different frequencies should be examined carefully whether they are really connected through any acceptable physical mechanisms and also originated from the same driving source or not. In general the frequency decreased, in other terms the period increased, in the frequency shift phenomenon appeared in our analysis of the averages of zonal winds over the tropics in connection with sunspot cycle. Hereafter, we will call the frequency shift as "red shift" in analogue with the gravitational red shift or the doppler red shift (Beiser 1969; Symon 1971).

By exhaustive and careful comparison of the wavelet analyses of the sunspot cycles and the seemingly corresponding oscillations in the zonal winds over the tropics, we found convincing evidences of the reality of the previously mentioned frequency shift, 'red shift' in general. The wavelet analysis gives the local power distribution in time and as a function of the frequency or periodicity. The method is ideal for the investigation of the power distribution of a time series as a function of frequency and local time. As the basis function for the wavelet analysis, we adopt 'Morlet' function which gives non-orthogonal complex wavelet transform. The non-orthogonal wavelet transform is good for the analysis of the time series characterized by the smooth and continuous variation of spectral power in time. The complex wavelet function is ideal for the analysis of oscillatory behavior, for it gives an amplitude and phase information simultaneously.

In summary, there might be some relations between the sunspots and selected meteorological variables locally and in a certain case globally, even though some authors claimed their no finding of relations. Even we accept the complication involved in the analysis methods and the differences of the parameters from the common or various data sets, there might exist so far unknown or fundamental limitations in our understanding of the phenomenon when meditating the opposite or inconsistent conclusions on the same subject from various data sets, in a certain case from the common data sets.

In this paper, we will concentrate mainly on the fundamental understanding of the atmospheric responses to oscillatory forcing by investigating sunspot cycle and related oscillatory motions observed in the meteorological variables rather than concerning with the direct relations between the fields of analysis, which were investigated and sought by many authors so far up to the present. We are not concerned with direct usage of the sunspot numbers for the climate prediction or the estimation of the agricultural crops, but we will try to understand how the oscillations induced by sunspot signals might change their frequency during the atmosphere responses. If such relationship comes to be clear, then we can deal with the related diverse problems without spending our energy and time in vain by avoiding brute force attacks on the subject.

This paper is composed of as follows. The following section describes the source of data and variables to be investigated. Section 3 has a simple introduction for the wavelet analysis methods. Section 4 deals with the observed aspects of the phenomena. In section 5 we give a theoretical aspect of the forced and damped harmonic oscillator and devised a calculation method for simulating the observed time series of 850 hPa zonal winds for showing one of the possible mechanisms of 'red shift' in the atmosphere. Finally we will talk about the conclusions and implications of our findings.

1. Data

The atmospheric data used in this study were obtained from the Climate Data Center of the National Oceanic and Atmospheric Administration (NOAA) of the United States. The monthly data have been downloaded from the data archive center announced on the web page cdc/reanalysis/reanalysis.html of the URL www.cdc.noaa.gov. The data based on National Centers for Environmental Prediction/the Department of Energy (NCEP/DOE) Atmospheric Model Intercomparison Project-reanalysis II comprise the various meteorological parameters at the seventeen standard pressure levels from 1000 hPa to 10 hPa as well as the surface flux values. The reanalysis II data is originally based on the National Centers for Environmental Prediction/National Center for Atmospheric Research (NCEP/NCAR) reanalysis I but with additional fixing of human processing errors and using updated forecast model and diagnostic packages that had been developed since the frozen of the reanalysis I system (Kanamitsu et al. 2002). For details on the forecast model and diagnostic packages for the reanalysis I, refer to Kistler et al. (2001) and Kalnay et al. (1996).

The zonal winds were separated from the downloaded data. By taking an area average of the zonal winds for a latitude belt from 15 °S to 15 °N in latitudes, we produced the area average value of the winds at each pressure level for a given month. The data period extends from January 1948 to June 2003, which has 666 sampling points with a time interval of one month.

Besides the zonal winds, two more variables are examined for their transient variations and inter-relationship, especially for the characteristics of power distribution in the frequency domain as a function of time. One of them is the sunspot numbers for the time period from January 1749 to July 2003 obtained from http://science.nasa.gov/ssl/pad/solar/sunsopts.html. According to a brief introduction on the web page, sunspot number is defined as the ten times of the number of sunspot groups plus the number of individual sunspots. Somewhat complex counting method for sunspot number may be compensated by the stableness of the numbers irrespective of the observation conditions in general. The sunspot data are the monthly averages and standard deviations derived by the NOAA, which are originally from the International Sunspot Numbers compiled by the Sunspot Index Data Center in Belgium. We processed the sunspot number data starting from 1866 by taking into account the period of the southern oscillation index (SOI) to be described in following paragraph.

In our comparison of the time series of sunspot numbers and the area averages of zonal winds, the data time period is pretty limited when considering the periodicity of the sunspot numbers of about 8-13 years. The limitation comes from the meteorological data that starts from year 1948. The realization is more or less five, which is obviously too short to evaluate the statistical significance for determination of the effects of sunspot cycle on the winds. In the mean time we found a very close relationship between the averaged zonal winds of 850 hPa and the SOI indices for the time period from 1948 to 2003. By taking into account a strong similarity between the temporal variations of the SOIs and the 850 hPa zonal winds, for comparison we extended the time period of the SOIs and the sunspot numbers backward to year 1866. The SOI data has been obtained from the ftp site ftp://ftp.cru.uea.ac.uk/data of the Climate Research Unit of University of Anglia in the United Kingdom. The data covers from 1866 to 2003 and are based on the SOI calculation method suggested by Ropelewski and Jones (1987).

As a visual check for the zonal winds and sunspot cycles, we prepared a plot for the time series of the both variables from January 1948 to June 2003. The sunspot cycles show oscillations with the mean period of about 11 years in Fig. 1a. The data starts from 1747 but we used the data for the time period after 1948 for conforming to the zonal winds starting from 1948. In Fig. 1b and 1c, the most notable one is annual cycle for the both winds. There exists a slower drift in time of the zonal winds toward large values, of which trend might be problematic for further analysis. The trend is more obvious for the 150 hPa winds than for the 850 hPa. However, the trend may have minor effects on the results of our analysis since we concern only with the oscillations with 11-year periodicities which are comparable with that of the sunspot cycles.

2. Wavelet analysis

The principal tool for our investigation is wavelet analysis. Basically there are two kinds of wavelet analysis according to what kind of wavelet functions are adopted for the wavelet transform. When one uses orthogonal set of wavelet functions for the transform, he is using the discrete wavelet transform. On the other hand, when one uses non-orthogonal wavelet functions, he can do discrete or continuous wavelet transform upon his requirement. Ours is the continuous transform using as the mother wavelet function the plane wave modulated with a Gaussian function. The orthogonal transform is more appropriate for the reduction of large data such as digitized images as commented by Koornwinder (1993). On the other hand, the continuous one, especially the Morlet wavelet, was preferred for the analysis of the meteorological variables (Meyers and et al. 1993; Weng and Lau 1994; Percival and Guttorp 1994; Torrence and Compo 1998). The most comprehensive work on the wavelet transform of meteorological variables is by Torrence and Compo (1998), of which functions and procedures were adapted properly for our analysis. In spite of their comprehensive work for the method, we still think that it is worthwhile to present some practical materials for understanding of the transform. The Morlet has real and imaginary parts. Its graphical form and Fourier transform function is given in Fig. 2. Its wavelet functions and necessary formula are given in table 1. Most of the practical materials have been quoted from Torrence and Compo (1998), and adapted if necessary.

According to the previous works on the advantage of the Morlet wavelet transform for meteorological variables are as follows. As the Morlet wavelet transform allows the continuous transform, we can select arbitrary scales for detailed analysis of the power distribution in the local period or frequency domain. In our analysis, we exploited such a feature to a full extent for deciding the exact value of period which has a local power maximum in the frequency domain at a given time. Smaller value of the scale interval gives a finer resolution in period or frequency. The scale interval was 0.125 for the most of our analysis and 0.0125 for the detailed distribution to determine the period of maximum power for the frequency bands of interest. The wavelet amplitude distribution resulted from the two different intervals of scale are not differentiable to a naked eye in comparison of the corresponding figures (not shown). However, the fine resolution in scale allows us to determine digitally the period of local maximum power.

As many people are accustomed with the frequency or periods when dealing with the oscillatory motions in general, we will use frequency or period instead of scale in our explanation of the periodic motions hereafter. The period, more specifically Fourier period, is related to the scale of the Morlet wavelet transform through the function given in Table 2. This relationship is different for individual wavelet transforms. For the Morlet transform with ω_0=6, the Fourier period has the relation, T = 1.03 s. There is a small difference in magnitudes between the Fourier period and the wavelet scale for the Morlet transform. The e-folding time is $\sqrt{2}\,s$ for Morelet wavelet transform. In contrast with the representation of Torrence and Compo (1998), we did not mark the area included in the cone of influence in our figures. For the periods of interest such as 10 years for the sunspot numbers and the 150 hPa zonal winds and 15 years for the 850 hPa winds, the e-folding times are 14 years and 21 years, respectively. We do not think that the end effects producing the cone of influence will significantly change the results of our statistical analysis because of the extended period of our data. For our wavelet analysis, we used the following specific values given in Table 2. Whenever those values are doubtful, we tried slightly different values from chosen values but did not come across any notable differences in the final wavelet transform.

We applied the wavelet analysis to the time series of the SOI, the sunspot number, and the zonal winds at all the standard pressure levels from 1000 hPa to 10 hPa. The Morlet wavelet transform has non-orthogonal wavelet functions which are useful for time series analysis, where smooth and continuous variations are expected in wavelet amplitudes. As the Morlet wavelet function is complex, it gives information about the both amplitude and phase of the analyzed time series, which is ideal for capturing oscillatory behavior.

4. The observed aspects

a. Sunspot numbers and the zonal winds

As expected from the unprocessed time series of the sunspot numbers shown in Fig. 1, the wavelet spectrum is dominated by about the 11-year cycle for sunspot number and annual cycle for the area averaged zonal winds at the 150 hPa and 850 hPa levels. These are also clear in the Fig. 3 displaying the real part of the wavelet coefficients. In contrast with the approximate 11-year cycle in the sunspot numbers, the zonal winds have distinct time variations of annual, semi-annual, and El-Nino periods. In addition to those frequency bands, we can point out 11-year cycle in the 150 hPa level winds and 15-year one in the 850 hPa winds. In global wavelet power, these bands have comparable intensity of power to the El-Nino component at each corresponding level. The oscillations of 850 hPa level may or may not be related to the sunspot cycle. Before anything else, we have to know the degree of relationship between the 850 hPa oscillations and the sunspot cycles. The discrepancy of the periods of the two wind oscillations forced us to examine the features of the 850 hPa winds in more detail.

When we draw the modulus of the wavelet transform for 5.5-31.17 year periods as in the figures of Fig. 4 for the sunspot numbers, the 150 and 850 hPa winds in order, we can point out with ease the relative maximum power at about the periods close to the sunspot cycles except for some deviations at 850 hPa in Fig. 4c. With such minor exceptions, the local maxima of relative power are clearly defined in the transform. In the case of the sunspot number, the end effects are somewhat degrading the power of the wavelet in the data period close to the both ends. The end effects exert the years close to the data ends according to the formula shown in Table. 2. The e-folding time coefficients are 14 years for the sunspot cycle and the 150 hPa winds and 19 years for the 850 hPa winds. Even though we do not exclude samples contaminated partly by the end effects, the decreasing trend of the power as we go back toward the beginning year of the sunspot number will be confirmed to be real in the extended data set, which will be shown in the following section. In contrast with the distribution of the modulus, the real coefficients as shown in Fig. 3 is free from the end effects because the zero valued contours in the distribution of the corresponding coefficients have the same shape irrespective of the magnitude of modulus.

As the wavelet transform gives power or amplitude distribution as a function of frequency and time, it allows us to examine the relationship between the frequency and the amplitude of maximum power as shown in Fig. 5. The amplitudes at the frequency of maximum power spread extensively in magnitude as the period of maximum power increases in general for the oscillations in the time series of all the three analyzed variables. The pattern simply reflects a large variation of the amplitudes of maximum power in the time domain, which is also discernable from Fig. 4. Such a temporal variation of the amplitude of maximum power may be very useful for identifying any or no connection of the zonal winds to sunspot cycle. In Fig. 6, the periods of maximum power for the 150 hPa and 850 hPa winds are inversely and directly proportional to the sunspot numbers, respectively, with minor exceptions. Such a reverse relationship for the both levels suggests the different driving mechanisms for the oscillations at the corresponding level. And similarly, the periods and the amplitudes of maximum power in the wavelet analysis of the 150 hPa and 850 hPa winds are also compared with respect to the amplitudes of maximum power of sunspot and displayed in Fig. 7. In the first figure of Fig. 7, the period of the 150 hPa winds decreases as the sunspot number increases. Such a tendency holds also for 850 hPa winds except for the outliers lying in the upper portion of Fig. 7b, which can be neglected safely by considering the fact that the 850 hPa winds have more power in the frequency range with periodicities shorter than 17 years in the global wavelet power spectrum (not shown). In addition to the above features, we can confirm a close connection of the zonal wind oscillations to the sunspot cycles in Figs. 7c and 7d, which show almost linear relationship between the amplitudes of the zonal winds and the sunspot cycles, except for the signature of saturation in the winds as sunspot number approaches to 700.

In Fig. 8a, the wavelet power of the zonal winds is concentrated on the 12-18 year bands except for the strong concentration of power around the annual, semiannual, and El-Nino cycles. And similarly the frequency bands of 11-16 years, a bit shorter than that of the 850 hPa zonal winds, are conspicuous in Fig. 8b. The distribution is almost the same as those of many other results based on the analysis of the SOI data such as Fig. 8 of Torrence and Compo (1998). At the first glance of the two figures of Fig. 8, there seems to be some fundamental differences for the time period from 1970 to 1980. A careful examination reveals that the detailed local distribution of the power is nearly the same except for a slight shift toward higher frequency regime in the SOI analysis than in the area averages of the 850 hPa zonal winds. Of course, the SOI has no annual and semiannual signals compared with the area averaged winds, which is understandable from the way of producing the incices.

b. Data extension

In Figs. 3c and 4c, we can observe the frequency bands with periods of about 12 years to 18 years. When investigating any probable relationship between the sunspot cycle and the oscillations represented by the band appeared in the figures, data period is not enough to make a final decision. From the reanalysis and sunspot data, we try to seek reliable evidences for the connection of the 850 hPa wind oscillations and the sunspot cycles. We have shown some findings, but we have only five realizations in a very restricted sense because of the limited data time span and relatively very long period of sunspot cycle. In order to reassure some aspects of the relations mentioned before, we examined the sunspot and SOI index data beginning at the year of 1866 (Fig. 9) instead of the 850 hPa winds dated back only to 1948. The SOI behaviors almost the same as the area average values of the zonal winds for the tropical belt for the NCEP data starting from 1948. We assumed that such tendency holds for the entire data period from 1866.

Figure 9 shows the distribution of amplitudes and real coefficients from the wavelet transform of the sunspot numbers and the SOI time series since 1866, respectively. The modulus and real coefficients of the sunspot were given in Figs. 9a and 9b, respectively. There exist changes in amplitude and frequency distribution with time interval of about

30-40 years, which are discernable in the figure (a) and somewhat less clearly from the real coefficients in (b). The feature may be also inferred from the time series of sunspot number in Fig. 1a which shows the sunspot numbers since 1948. The years with relatively broad local spectrum of 1890, 1920, 1960, and 1990 in the wavelet transform have very large amplitudes and very rapid change of the number with time in the unfiltered sunspot numbers. The sunspot number time series are not shown for the entire period but the previous mentioned feature can be confirmed for the last half of data period from Fig. 1a. In addition to the above feature, the most notable aspect is the strong signature of large amplitude of the wavelet power after 1940 in the sunspot numbers. In correspondence with such a change of sunspot number, we can point out easily the overall frequency shift by about 2 years from the 12-18 year period to the 10-16 year period of the SOI variation, as denoted roughly with the rectangles of solid line for the time period before 1940 and of dashed line after that year in Fig. 9c. The changes in the figure seem to suggest that the amplitude of the sunspot variation had direct impacts on the oscillations in the SOI in a broad sense. For each sub-period of data, the periods of the oscillations decrease in time slowly. The reason of such a drift of the frequency of local maximum is not clear yet. The topic will be dealt with in future.

5. Interpretation

a. Basic theory

From our careful analyses of the features of the oscillations in the area average values of the zonal winds in the upper and the lower troposphere, we showed that the oscillations had a close connection with the sunspot cycles and they seemed to be independently driven by the sunspot cycles rather than that the upper oscillation induces the lower one or vice versa. For interpretation of the possible connections of the seemingly disconnected features to the conventional viewpoint which has been established largely from correlation statistics, we adopted the behavior of the forced and damped harmonic oscillator and frequency modulation technique. A schematic for the damped harmonic oscillator is given in Fig. 10. It is well known that the oscillatory motions of a simple harmonic oscillator will have a longer period or smaller frequency compared with its natural frequency when damping is working on. The solution of the differential equation for the oscillator is dependent on the initial condition of the system. In mathematical terms, it is the initial value problem.

In an actual case, the homogenous solution of the above mentioned system will die out soon as time goes on because of damping irrespective of its sources. If we loose the condition of the forced damping oscillator for its solutions, we can adopt the oscillator as the conceptual model for the case of the sunspot cycles and the atmosphere responses to them. In general the forced oscillator is driven by solely the driving frequency, in our case the sunspot period. The period is well matched to the zonal wind at the upper atmospheric layer centered at 150 hPa level. The amplitude of the responses decreases rapidly as one goes up or down form the level along the vertical direction. In the lower troposphere with maximum amplitudes centered at 850 hPa level, the period of the oscillations increase by about three years with respect to that of the upper level oscillation. The difference may arise mainly from the different magnitude of frictional damping in the both layers. We might expect more damping in the lower troposphere than in the upper troposphere. The actual mechanism for damping should be clarified but the topic seems to be beyond the scope of our present work.

In our trial of applying a harmonic oscillator for frequency shift, we have to estimate the natural frequency of the atmosphere layer concerned. At the present, we simply assume that the upper oscillation is virtually in a resonant state with the sunspot cycle. In our assumption, no infinite growing of the amplitude of the upper oscillation may be due to the nonlinear effects in the amplification of the amplitudes or other damping factors related to friction or other nonlinear processes so far unknown dynamical and/or physical processes involved.

By considering the relatively small friction in the upper atmosphere and so small frequency deviation from the sunspot period, we will use the value of the observed frequency of the upper oscillations as the natural frequency of the atmosphere. The exact method of estimating or measuring the natural frequency of the atmosphere layer will become a future research topic in this trail of searching the effects of sunspot cycle on the atmosphere.

The damped harmonic oscillator may be described as,

$$\ddot{S}(t) + \Gamma \dot{S}(t) + \omega_0^2 S(t) = \omega_0^2 S_d e^{-i\omega_d t} , \qquad (1)$$

The symbols in the above and the following equations are: $S(t)$ and $S_d(t)$ denote the status of responding and forcing systems, Γ friction, ω_0 and ω_d the natural and forcing angular frequencies, the symbol dot means time differentiation. The complete solution of equation (1) may be written as,

$$S(t) = S_{homo}(t) + S_{forced}(t) . \qquad (2)$$

The homogeneous and forced parts of the solution are as follows,

$$S_{homo}(t) = e^{-\frac{\Gamma}{2}t}\{c(t)\cos(\omega t) + d(t)\sin(\omega t)\}\,, \tag{3a}$$

$$\begin{aligned} S_{forced}(t) &= \frac{\omega_0^2(\omega_0^2 - \omega_d^2)^2 S_d}{(\omega_0^2 - \omega_d^2)^2 + \Gamma^2\omega_d^2}\cos(\omega_d t) + \frac{\Gamma\omega_d\omega_0^2 S_d}{(\omega_0^2 - \omega_d^2)^2 + \Gamma^2\omega_d^2}\sin(\omega_d t) \\ &= \frac{\omega_0 S_d}{\Gamma}\sin(\omega_d t)\,. \end{aligned} \tag{3b}$$

In contrast with examples in a general mechanics text book (e.g., Symon 1971; Georgi 1993), we have to consider the two types of solution at the same time to show the frequency shift phenomenon, red shift. Therefore, the constants c and d are actually dependent on the starting time of the free oscillation in our treatment. The second expression for the forced solution is possible by assuming $\omega_0 = \omega_d$. The magnitude of Γ in the lower troposphere is estimated from the assumptions: the natural frequency ω_0 is the same for the upper and lower troposphere, the observed frequency represents that of the damped oscillator, and the upper atmosphere Γ is set to be zero. The practical way of producing the time series simulating the 850 zonal winds will be given in the following section.

b. Marginal driving force

To check the validity of our assumptions, we produced time series resulted from the damped harmonic oscillator with intermittent forcing rather than continuous driving force which is regarded as quite a natural in numerous mechanics text book (e.g., Georgi 1993). For the continuous forcing, the homogenous solutions will die out ultimately and the driving frequency will dominate the system in time invariant fashion.

In our case of intermittent forcing, we have to consider the both types of solution at the same time. For the intermittent forcing we assume that the solution may be composed as shown in Fig. 11. The starting time is not important. The relative length of forcing and the attenuation time scale is crucial to determine the frequency characteristics of the produced time series. Determination of the time period of forcing will be explained later.

For a time step i , the composite solution is composed with as following for the various time spans. The index i goes from 0 to *I*, where *2I*+ 1 should be less than the total time step N.

$$
\begin{aligned}
S_G^i(t) &= (1-\frac{t-t_{2i}}{\tau})S_{homo}(t-t_{2i-1}) + (\frac{t-t_{2i}}{\tau})S_{forced}(t) && \text{for } t_{2i} \langle\, t \le t_{2i}+\tau \\
S_G^i(t) &= S_{forced}(t) && \text{for } t_{2i}+\tau \langle\, t \le t_{2i+1} \qquad (4) \\
S_G^i(t) &= S_{homo}(t-t_{2i+1}) && \text{for } t_{2i+1} \langle\, t \le t_{2i+2}
\end{aligned}
$$

In the first equation, the homogeneous part $S_{homo}(t-t_{2i-1})$ should start at time $t = t_{2i-1}$. Therefore, time dependent constants $c(t)$ and $d(t)$ of the homogeneous solution should be determined at time $t = t_{2i-1}$ for index $i-1$. The determination of $c(t_{2i-1})$ and $d(t_{2i-1})$ will follow soon.

The homogeneous solution for the time interval t_{2i+1} to t_{2i+2} is,

$$S_G^i(t, t_{2i+1}) = e^{-\frac{\Gamma}{2}(t-t_{2i+1})}[c(t_{2i+1})\cos\{\omega(t-t_{2i+1})\} + d(t_{2i+1})\sin\{\omega(t-t_{2i+1})\}]\,, \tag{5}$$

and its differentiation is,

$$\begin{aligned} \dot{S}_G^i(t, t_{2i+1}) = &-\frac{\Gamma}{2} e^{-\frac{\Gamma}{2}(t-t_{2i+1})}[c(t_{2i+1})\cos\{\omega(t-t_{2i+1})\} + d(t_{2i+1})\sin\{\omega(t-t_{2i+1})\}] \\ &-\omega e^{-\frac{\Gamma}{2}(t-t_{2i+1})}[c(t_{2i+1})\sin\{\omega(t-t_{2i+1})\} + d(t_{2i+1})\sin\{\omega(t-t_{2i+1})\}]\,. \end{aligned} \tag{6}$$

For the expression in the left-hand side of the equations (5) and (6), the second argument t_{2i+1} in parenthesis means the initial time for the solution. At time $t = t_{2i+1}$, the above expression can be reduced to

$$\begin{aligned} S_G^i(t_{2i+1}) &= c(t_{2i+1})\,, \\ \dot{S}_G^i(t_{2i+1}) &= -\frac{\Gamma}{2} S_G^i(t_{2i+1}) + \omega\, d(t_{2i+1})\,. \end{aligned} \tag{7}$$

Finally,

$$\begin{aligned} c\,(t_{2i+1}) &= S_G^i(t_{2i+1}) \\ d\,(t_{2i+1}) &= \frac{1}{\omega}\{\dot{S}_G^i(t_{2i+1}) + \frac{\Gamma}{2} S_G^i(t_{2i+1})\}\,. \end{aligned} \tag{8}$$

Time dependent constants $c(t_{2i+1})$ and $d(t_{2i+1})$ determined at the time step

i ($t = t_{2i+1}$) will be used for the homogeneous solution in the next time step $i+1$ ($t = t_{2i+3}$). In the procedure, the most important factor is driving time and duration. We already commented frequency and amplitude modulations in Fig. 9a. There are some effects of the variations of amplitude and damping on the frequency shift, but these are not so critical to control the frequency character of the produced time series.

When we modulated the 10-year periodicity time series with 30-year frequency modulation, we have time series shown in Fig. 12b. The equation for frequency modulation is as following.

$$SSN_{\text{mod}} = A\sin(\omega_0 t + \phi_{\text{mod}} \sin \omega_{\text{mod}} t), \tag{9}$$
$$\phi_{\text{mod}} = k\eta / \omega_{\text{mod}}.$$

In the above expression, the modulation index ϕ_{mod} decides the fundamental feature of the modulated time series. In order to have a sense on sensitivity of produced time series for various values of the index, we produced many modulated time series with various values of the index. In a one sinusoidal harmonic component case, the modulation index decides the relative amplitude of the carrier wave and the side bands. We tried the sinusoidal case because of intractable complexities of frequency modulation for general case as cautioned by Thomas (1989). When we applied 12 for the modulation index by assuming $k = 2\pi$ and $\eta = 0.4$ for the given angular frequency of modulation $\omega_{\text{mod}} = 2\pi / 30$ (rad/years), the amplitude of the carrier wave is less than one third of that of the side bands approximately. The value for the modulation index seems to be a bit larger in our simulation than in the real situation. However, any proper values can be assigned to k and η by Thomas (1989). The notable side bands are just two in our calculation: the upper sideband with periodicity of 15 years and the lower one of about 3-year period. The values of the required parameters in simulating the 850 hPa winds were summarized in Table 3 given in the previous section.

By assuming that the lower troposphere of the atmosphere was in a state to be able to respond to the sunspot cycles only when the driving frequency is lower than the characteristic frequency of the receiver, i.e., the lower troposphere layer, we have produced the modulated time series and associated analyses and displayed them in Fig. 12. The composite solution based on the modulated time series does show some similarities to the low frequency component of the modulated time series. From the figures, we can ascertain that a one harmonic component can produce a pretty complex wavelet pattern due to frequency shift and also that the low frequency component may emerge naturally from frequency modulation. Figure 12e shows that the 11-year cycle has still some power against the modulation. However, our simple calculation for a one harmonic component should be interpreted with a caution in applying to the real world case because of high abstraction of the relationship between sunspot and the oscillations of the winds in the atmosphere.

Even though we did not find the frequency bands probably arising from frequency modulation in the wavelet transform of the sunspots, it is worthwhile to look at carefully the power distribution around 1930-1940 in Fig. 9a. In the figure, there exists a clear suppression of oscillations with periodicities of about 13 years or longer. We think that the above suppression may be related to the notably reduced power of about 15-year period for the same period in the SOIs shown in Fig. 9c, rather than occurred by chance.

6. Conclusions

With some ad hoc assumptions for the application of the harmonic oscillator to our interpretation of relationship between sunspot cycle and probably associated oscillations in the troposphere, the damped and forced oscillator gives satisfactory answers to many aspects emerged in our wavelet analysis of the zonal winds. Even though our results can not be compared directly with other previous works dealing with sunspot cycle and seemingly related oscillations in the meteorological variables because of the different variables analyzed and the concerned regions of analysis on the earth, based on our analysis and simulation we would like to point out the undeniable limitations of some of the previous workers who adopted the coefficients of simple linear correlation statistics for the investigation of the sunspot effects on the atmosphere. The situation is almost the same for the application of the cross spectrum and/or the empirical orthogonal function analyses and other methods in this trail. Sometimes the approach will work out but would collapse soon for the occurrence of frequency shift such as 'red shift' as revealed in our analysis. In addition to the above mentioned limitation, we want to summarize our findings as follows.

Sunspot number has dominant periodicity of about 11 years without any other notable frequency bands with a relative maximum power in the frequency domain. The dominant frequency is not fixed in time but experiences a good deal of temporal variation with a modulation period of about 30 years. The feature may be called frequency modulation. At the same time the amplitudes of the dominant frequency also manifests amplitude modulation with almost the same length of period as for frequency modulation. These modulations are evident in Fig. 9.

The above mentioned both modulations might control the effects of sunspot on the weather, but the fundamental one seems to be frequency modulation, which would excite the oscillations in the lower troposphere winds with periodicity of about 15 years as shown in our simulation and analysis of the wind variations. The observed 13-18 year oscillations in the 850 hPa zonal winds are apparently forced by the sunspot related forcing but the observed frequency seem to be determined by the internal dynamics of the lower troposphere rather than by the frequency of external forcing in other terms sunspot cycle.

The 850 hPa zonal winds show temporal variation very similar to that of the SOIs, except for the large wavelet power in the annual and semiannual frequency bands, which is evident in Fig. 8 and also discernable from comparison of Figs. 3c and 9c. Such similarity is fully exploited for the increase of reliability in comparing the sunspot cycles to the 850 hPa zonal winds.

The zonal winds were controlled by the sunspot cycle in the upper troposphere for the oscillations with periodicities of about 8-13 years with a dominant 11-year period. The role of friction in the upper troposphere can be recognizable from the relative change of the periods of the oscillations in the sunspot and 150 hPa winds when moving away from the center portion of the analysis time in Figs. 3 and 4. In the lower troposphere, the oscillations seem to be controlled by the modulated sunspot cycles in combination with the friction of the lower troposphere. Their periods were 13-18 years with a center frequency of about 15 years, approximately. These facts may be explained with ease by assuming the difference of friction in strength in the both layers of the troposphere.

When comparing the SOIs and sunspot cycles, there was a close connection between their temporal variations. The magnitude of the sunspot numbers increased greatly when passing the year of 1940. At the same time the real coefficients of the wavelet transform of the SOIs are very different in their magnitude and distribution before and after 1940 in Fig. 9. In the figure, the approximate periodicities for the time span before and after 1940 are about 16 years and 14 years, respectively.

For our simulation of the 850 hPa zonal winds forced by a simple harmonic component, we estimated the natural frequency and friction by comparing the observed periods of the oscillations in the upper and the lower troposphere. We think that more direct method of estimating these parameters should be devised from deep understanding on the relations between the forcing and respondents. As the observed winds for the corresponding frequency bands in the troposphere can not be explained with a one harmonic component, we must deal with multi-frequencies manifesting frequency and amplitude modulations at the same time for more advanced understanding of the problem.

In future we will think about how to take into account the frequency and amplitude modulations at the same time in the investigation of any connections between the driving and responding oscillations. And what is the spatial structure of meteorological variables related with the zonal winds and sunspots. Some of them were examined by van Loon and Labitzke (1998) for the global troposphere and stratosphere in connection with sunspot cycle. Their results may be combined with ours to illuminate the sunspot related circulation changes in the atmosphere in future.

Finally our findings and conceptual model should not be considered as a unique answer to sunspot cycle and its effects on the earth atmosphere. On the contrary, our findings force us to make a new start for in-depth study of the oscillations originated from the internal dynamics and/or external forcing and their remotely forced oscillations. The related previous analyses and exclamation should be reexamined in context with frequency shift. The responding mechanism of the atmosphere to sunspot cycle should be investigated carefully. The variables and the affected regions should be expanded continuously in future. Our conceptual model has temporary assumptions for application. Their meaning should be clarified and the values of the parameters are to be estimated with the aid of a deep insight on the system in future. And also the oscillations generated from the internal dynamics or external forcing and the remote responses to them in other parts of the atmosphere should be examined as for the sunspot cycles and the related oscillations as done in our study.

Acknowledgements. This work was carried out as one of the many activities for the SSMG (NRL), which has been being supported by the National Science and Engineering Administration of the Republic of Korea since the year of 2001. The authors would like to express their sincere thanks to the graduate students, Baek-Min Kim and Mi-Kyoung Sung, of the SSMG who understood their requirements and made beautiful figures.

REFERENCES

Bain, W. C., 1975: The power spectrum of temperatures in central England. *Quart. J. Roy. Meteor. Soc.*, 102, 464-466.

Beiser, A., 1969: *PERSPECTIVES OF MODERN PHYSICS.* McGraw-Hill, 608 pp.

Dyer, T. G. J., 1976: An analysis of Manley's central England temperature data. *Quart. J.*

Roy. Meteor. Soc., 102, 871-878.

Georgi, H., 1993: *THE PHYSICS OF WAVES.* Prentice Hall, 422 pp.

Gerety, E. J., J. M. Wallace, and C. S. Zerefos, 1977: Sunspots, geomagnetic indices and the weather: A cross-spectral analysis between sunspots, geomagnetic activity and global weather data. *J. Atmos. Sci.*, 34, 673-678

Hancock, D. J., and D. N. Yarger, 1979: Cross-spectral analysis of sunspots and monthly mean temperature and precipitation for the contiguous United States. *J. Atmos. Sci.*, 36, 746-753.

Kalnay, E., and Coauthors, 1996: The NCEP/NCAR 40-Year Reanalysis Project. *Bull. Amer. Meteor. Soc.*, 77, 437-471.

.

Kanamitsu, M., and Coauthors, 2002: NCEP-DOE AMIP-II REANALISYS (R-2). *Bull. Amer. Meteor. Soc.*, 83, 1631-1643.

Kim, S. S., 1976: A Study on Summer Precipitation and Winter Temperatures at Seoul. *J. of Kor. Met. Soc.*, 12, 1-5

Kistler, R., and Coauthors, 2001: The NCEP/NCAR 50-Year Reanalysis: Monthly means CD-ROM and documentation. *Bull. Amer. Meteor. Soc.*, 82, 247-267.

Koornwinder, T. H., 1993: The Continuous Wavelet Transform. *Wavelets: An Elementary Treatment of Theory and Applications*, Ed. T. H. Koornwinder, World Scientific Publishing Co., 27-48

Labitzke, K., and H. van Loon, 1993: Some recent studies of probable connections between solar and atmospheric variability. *Ann. Geophys.*, **11**, 1084-1094.

___, and ___, 1995: Connection between the troposphere and stratosphere on a decadal scale. *Tellus*, **47A**, 275-286.

Lanzante, J. R., 1980: Comments on "Cross-Spectral Analysis of Sunspots and Monthly Mean Temperature and Precipitation for the Contiguous United States." *J. Atmos. Sic.*, **37**, 1138-1138.

Manley, G. 1974: Central England temperatures: Monthly means 1659 to 1973. *Quart. J. Roy. Meteor. Soc.*, **100**, 389-405.

Meyers, S. D., F. G. Kelly, and J. J. O'Brien, 1993: An introduction to wavelet analysis in oceanography and meteorology: With application to the dispersion of Yanai waves. *Mon. Wea. Rev.*, **121**, 2858-2866.

Moon, Y.-S., and S.-E. Moon, 1981: The Relationships of Sunspot Numbers and Temperature, Pressure and Precipitation in the Southern Part of Korean Peninsula. *J. of Kor. Met. Soc.*, **17**, 12-17.

Percival, D. B., and P. Guttorp, 1994: Long-Memory Processes, the Allan Variance and Wavelets. *WAVELETS IN GEOPHYSICS*, Ed. E. Foufoula-Georgiou and P., Kumar, Academic Press, 325-357.

Ropelewski, C. F., and Jones, P. D., 1987: An Extension of the Tahiti-Darwin Southern Oscillation Index. *Mon. Wea. Rev.*, 115, 2161-2165.

Shapiro, R., 1975: The variance spectrum of monthly mean central England temperatures. *Quart. J. Roy. Meteor. Soc.*, 101, 679-681.

Symon, K. R., 1971: *MECHANICS, third edition*. Addison-Wesley Publishing Company, 639 pp.

Thomas, J. B., 1989: Information, Communication, Noise, and Interference. Section 4 of *Electronics Engineer's Handbook*, Ed. D. G. Fink, and D. Christiansen, McGraw Hill, 4-1-4_50.

Torrence, C., and G. P. Compo, 1998: A practical guide to wavelet analysis. *Bull. Amer. Meteor. Soc.*, 79, 61-78.

van Loon, H., and K. Labitzke, 1990: Association between the 11-year solar cycle, the QBO and the atmosphere. Part IV: The Stratosphere, not grouped by the phase of the QBO. *J. Clim.*, 3, 827-837.

___, and ___, 1994: The 10-12 year atmosphere oscillation. *Meteor. Z.*, 3, 259-266.

___, and ___, 1998: The Global Range of the Stratosphere Decadal Wave. Part I: Its Association with the Sunspot Cycle in Summer and in the Annual Mean, and with the Troposphere. *J. of Climate*, 11, 1529-1537.

Weng, H., and K.-M. Lau, 1994: Wavelets, period doubling, and time-frequency localization with application to organization of convection over the tropical Pacific. *J. Atmos. Sci.*, 51, 2523-2541.

Table Captions

Table 1. The Morlet wavelet basis function and its properties. Constant factors for Ψ_0 and $\hat{\psi}_0(\eta)$ ensure the total energy of unity. Adapted from the table 1 of Torrence and Compo (1998).

Name	$\psi_0(\eta)$	$\hat{\psi}_0(s\omega)$	e-folding time τ_s	Fourier period
Morlet (ω_0 =freq.)	$\pi^{-1/4}e^{i\omega_0\eta}e^{-\eta^2/2}$	$\pi^{-1/4}H(\omega)e^{-(s\omega-\omega_0)^2/2}$	$\sqrt{2}\ s$	$\frac{4\pi s}{\omega_0+\sqrt{2+\omega_0^2}}$

Table 2. Empirically derived factors for the Morlet wavelet function. Parameters for processing monthly data for 1948-2003 period. The j and δj values in parenthesis are for more precise determination of the period of maximum power. Adapted from Torrence and Compo (1998).

Name	C_δ	γ	δj_0	$\psi_0(0)$	δj	δt	n	j
Morlet (ω_0 =6)	0.776	2.32	0.60	$\pi^{-1/4}$	0.125(0.0125)	1./12.	666	0:67(0:775)

Table 3. The parameter values used for the simulation of the 850 hPa winds. For feasibility, we use year as the unit for each parameter. The values of frequency or angular frequency may be evaluated from the corresponding periods with appropriate formula. The unnecessary values have been omitted.

	P (years)	P_0 (years)	P_d (years)	$\frac{2}{\Gamma}$ (years)	P_{mod} (years)
Sunspot	10		10		30
150 hPa	10	10		0	
850 hPa	15	10		3	

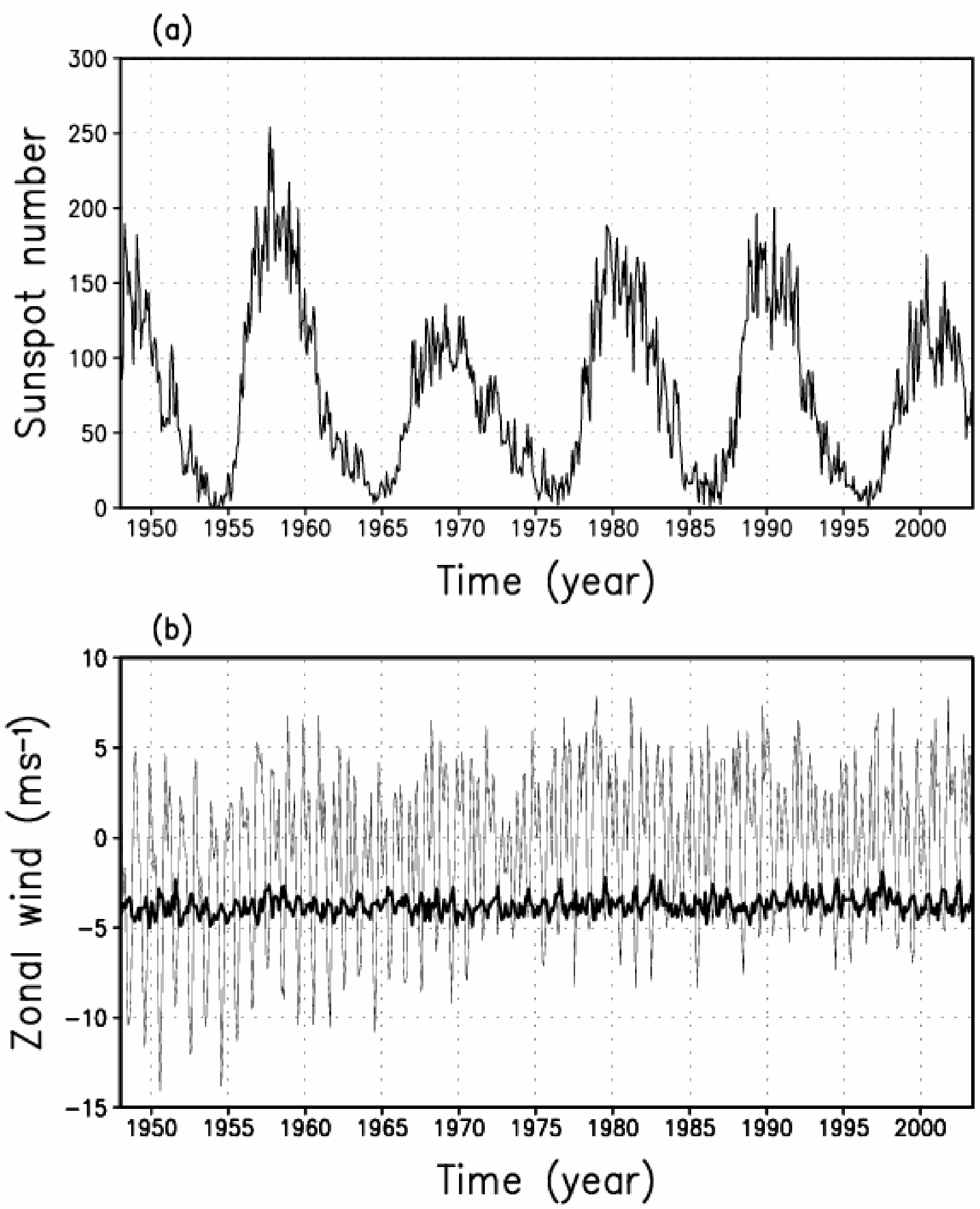

Fig. 1. Time series of (a) the sunspot numbers and (b) the 150 hPa winds in a thin line and the 850 hPa winds in a thick line for the data 1948-2003. The winds are based on the area averages of the zonal winds over the tropical belt extending from 15 °S to 15 °N in latitudes.

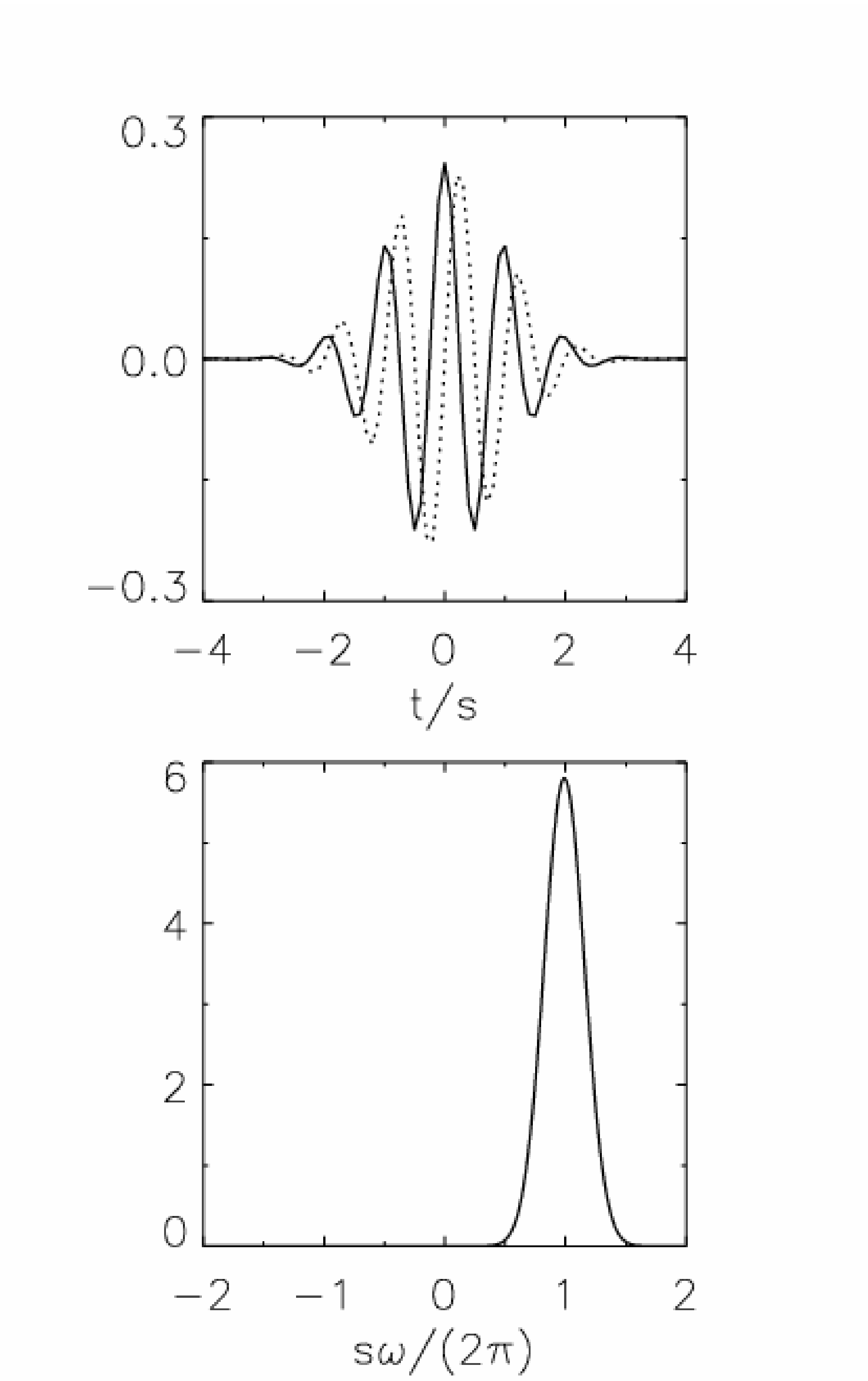

Fig. 2. The shape of the Morlet wavelet basis functions in real part (a) and in imaginary part (b). For drawing, the scale was chosen to be $10\,\delta t$. Adapted from Torrence and Compo (1998).

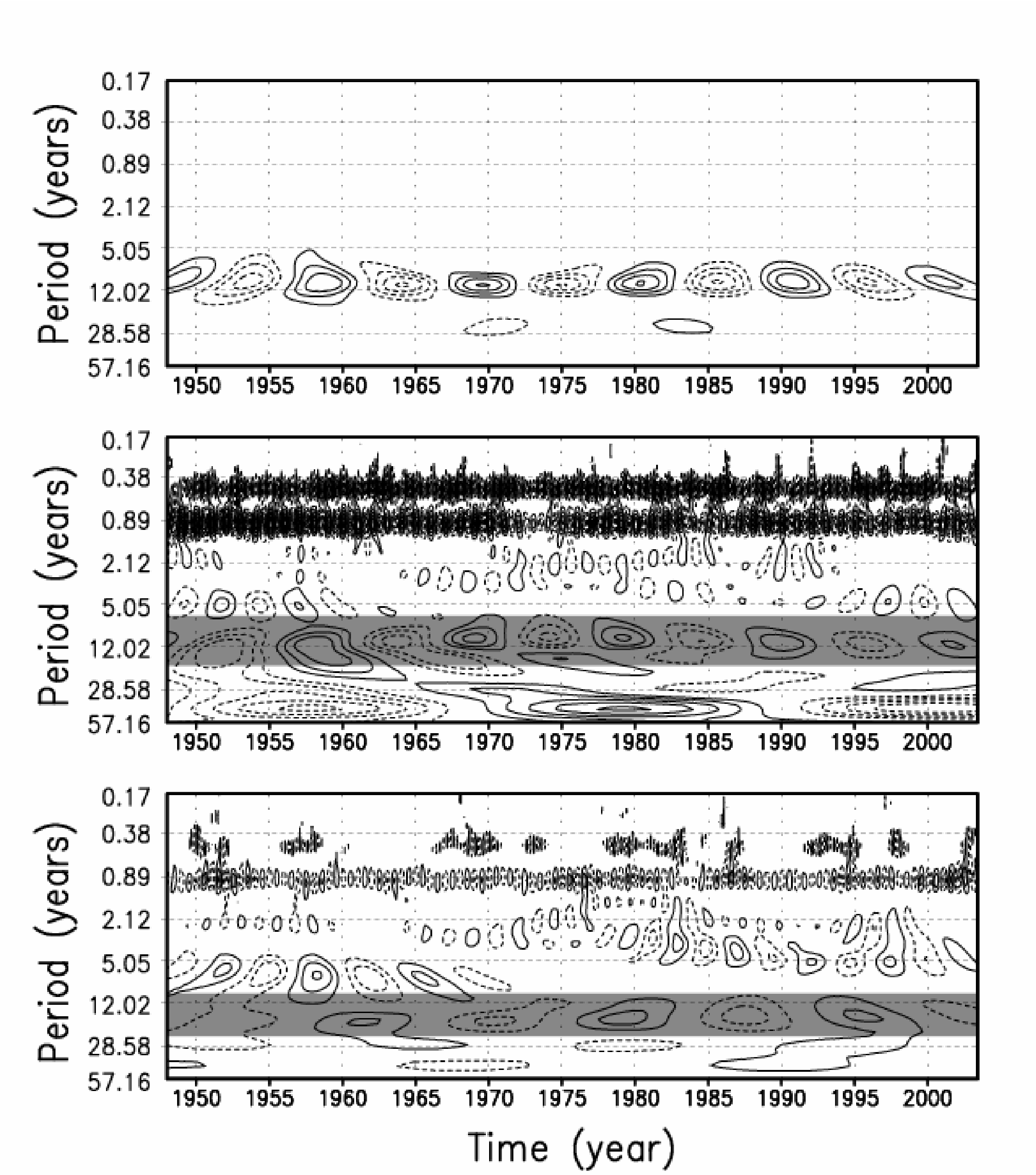

Fig. 3. The real part of the wavelet transforms of (a) the sunspot numbers, (b) the averages of the 150 hPa zonal winds, and (c) that of the 850 hPa zonal winds. The analysis time period covers from 1948 to 2003. The contour interval is 200, 10 m/sec, and 0.3 m/sec in order from top to bottom. In (b) and (c), the strip of shading denotes the approximate frequency bands closely related to the sunspot cycle. The center frequencies of the bands are 10 years and 15 years in order, approximately. The contour labels are omitted for clarity.

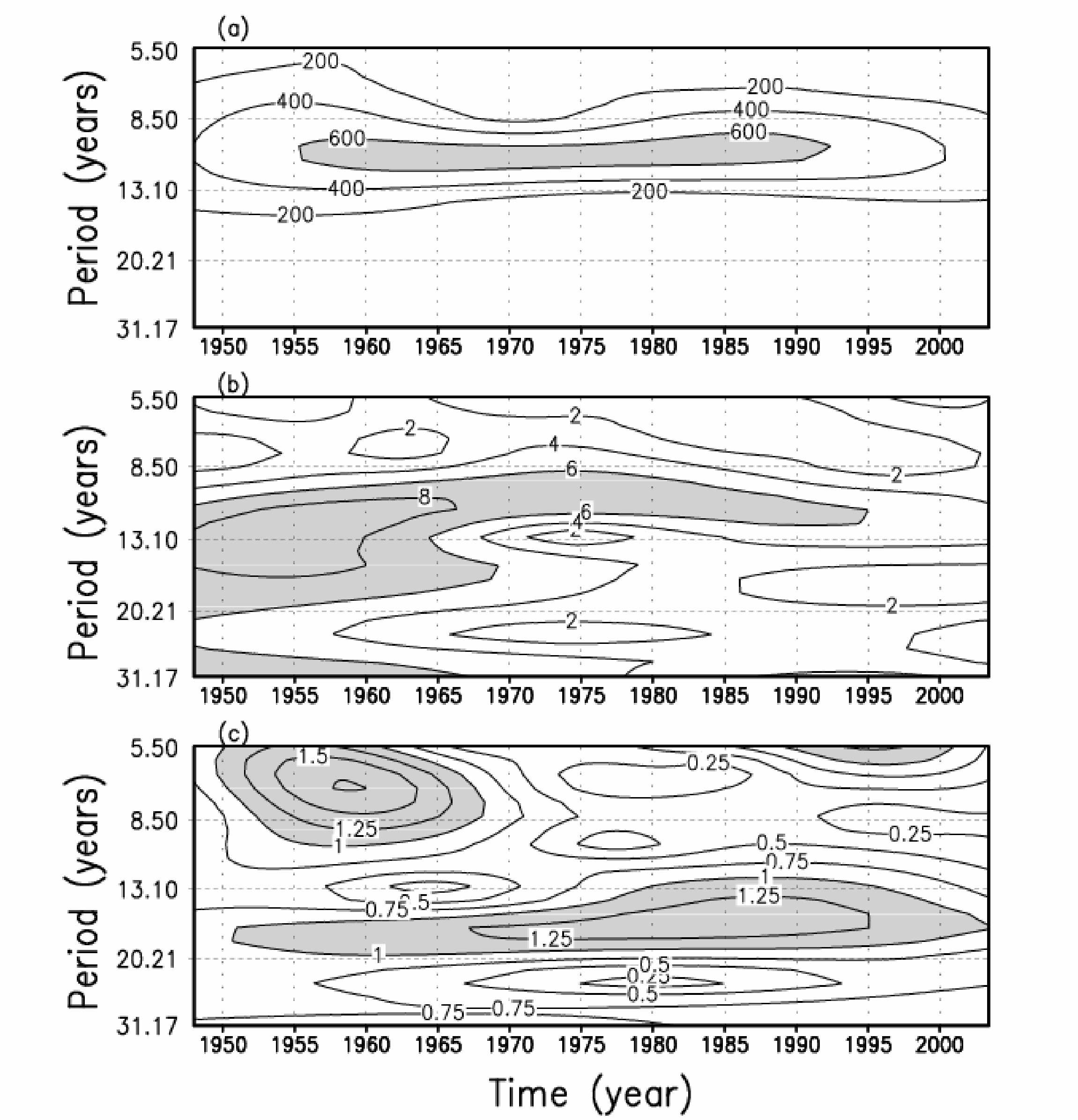

Fig. 4. The amplitude of (a) the sunspot numbers, (b) the 150 hPa winds, and (c) the 850 hPa winds in the wavelet transform for the period 1948-2003. Contour interval is 200 for (a), 2 m/sec for (b), and 0.25 m/sec for (c). The shaded area is for amplitudes larger than 600, 1.5 m/sec, and 2 m/sec for figures (a), (b), and (c) in order.

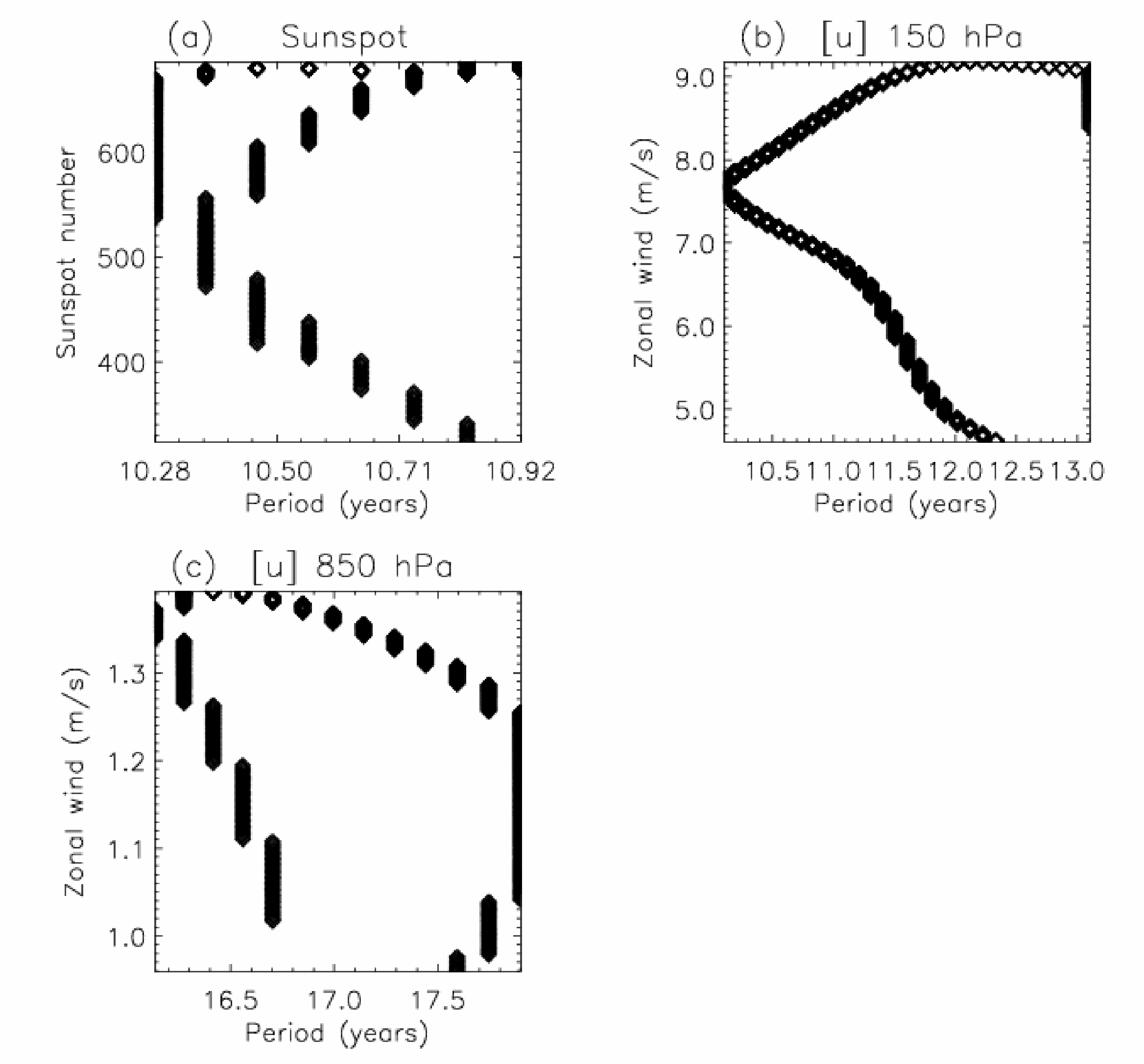

Fig. 5. The scatter diagram based on the amplitudes versus the periods of maximum power for all data samples of (a) the sunspot numbers, (b) the 150 hPa and (c) the 850 hPa winds, respectively.

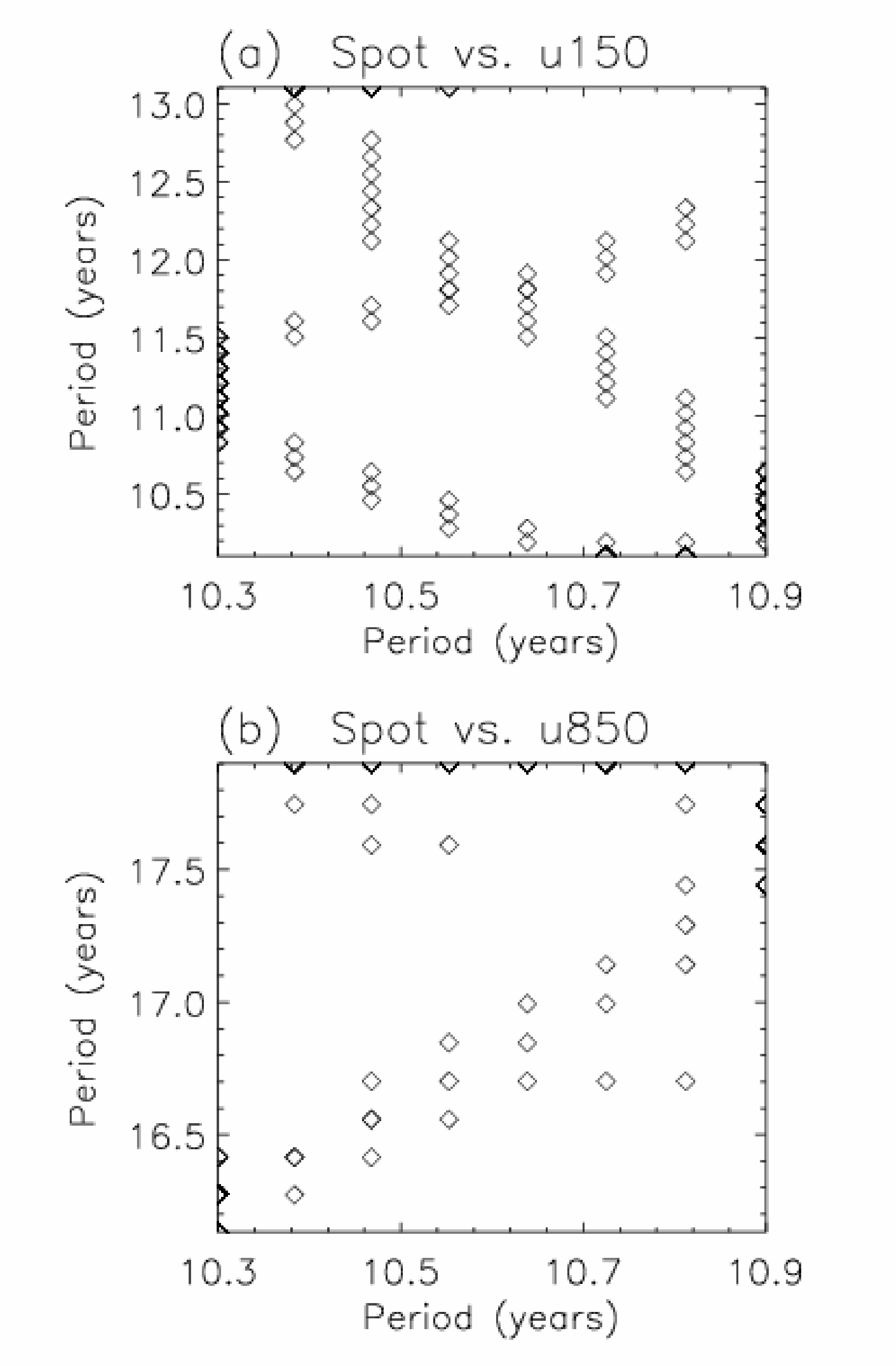

Fig. 6. The scatter diagram of the periods of maximum power for (a) the 150 hPa and (b) the 850 hPa winds with respect to those of the sunspot numbers. The period of maximum power has been searched only for the frequency band from 5.5-31.17 years to prevent the automatic selection of the periods of maximum related to the semiannual,, annual, and El-Nino variations.

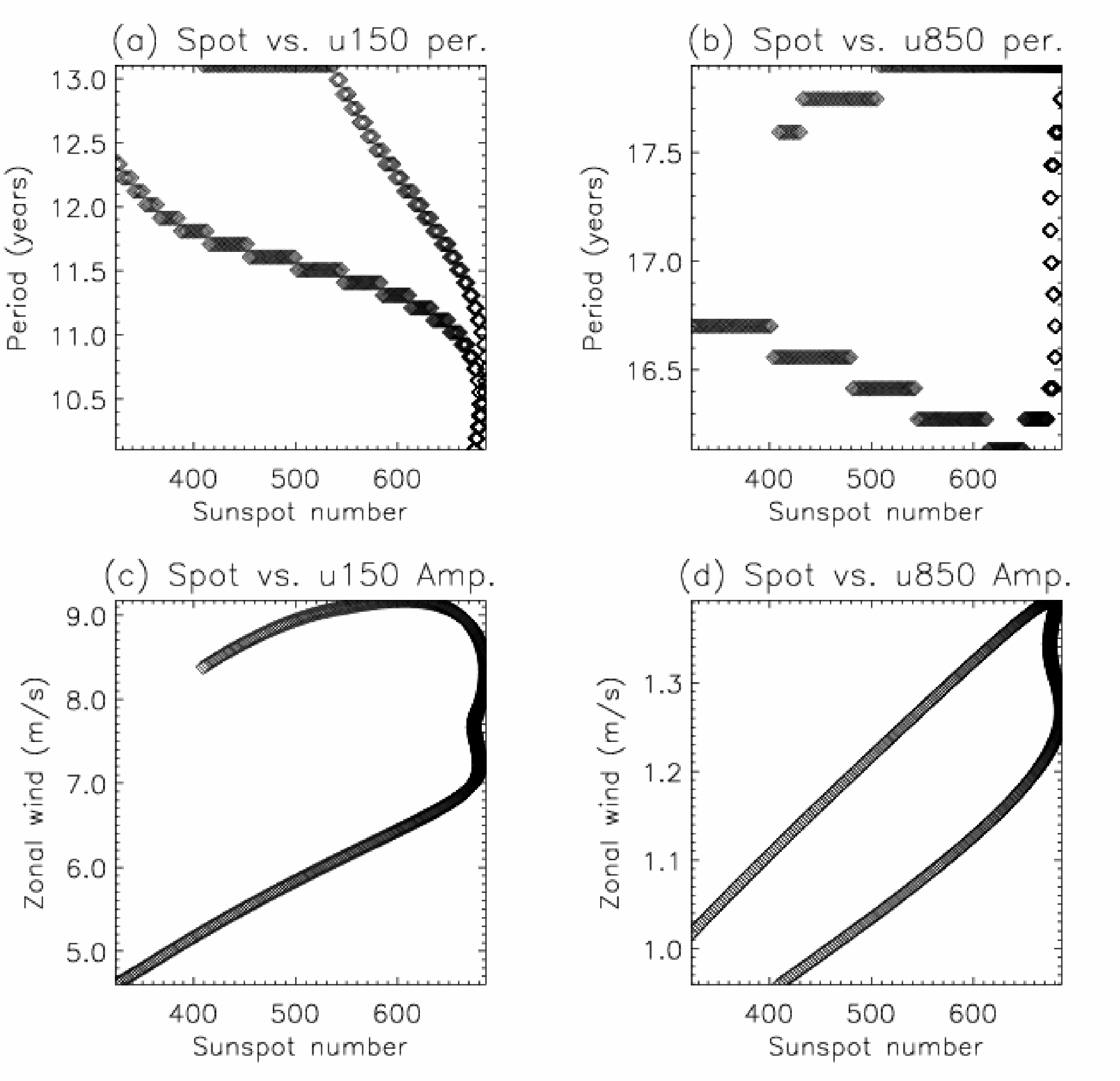

Fig. 7. The scatter diagram of (a and b) the periods of maximum power and (c and d) the amplitudes at the periods of maximum power in the wavelet transforms of the 150 hPa and 850 hPa winds with respect to the wavelet sunspot amplitudes at the corresponding periods for the entire samples.

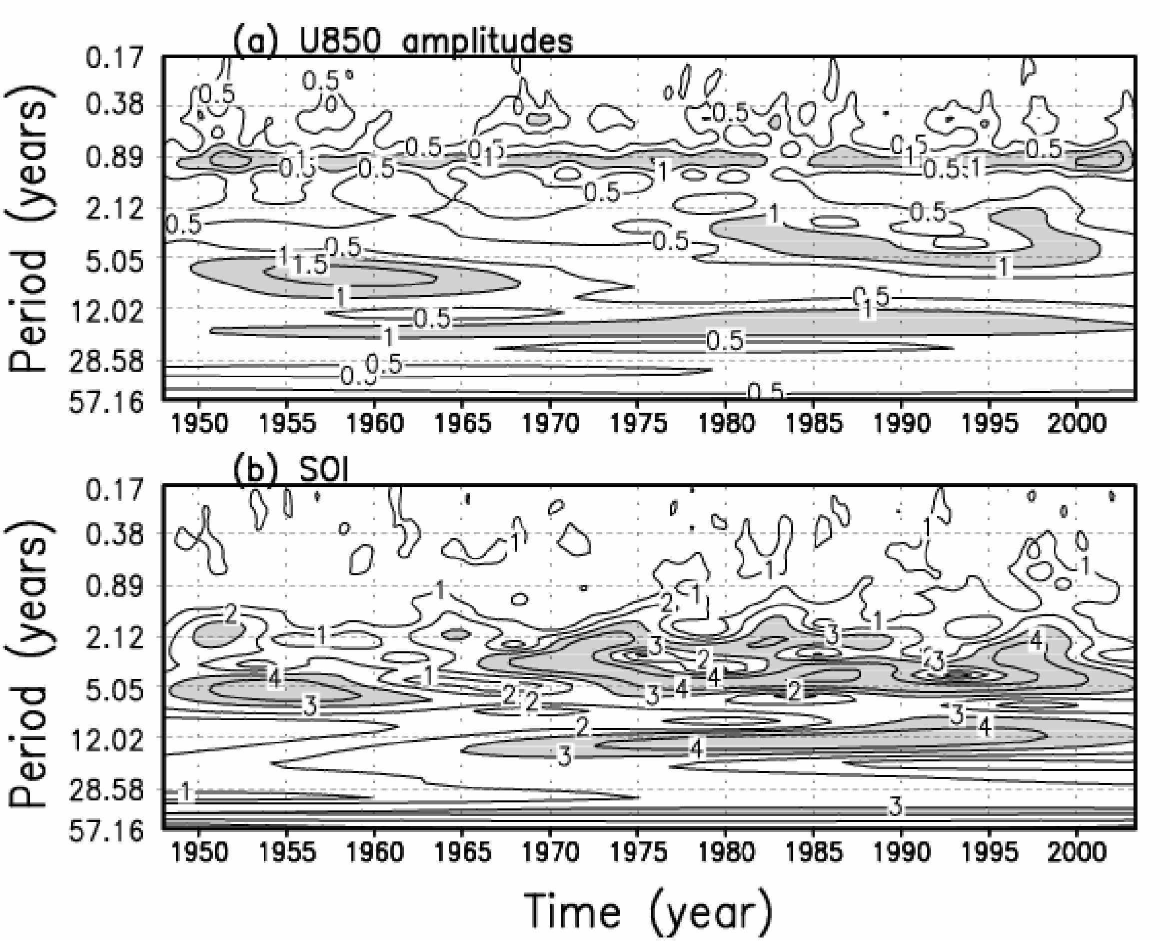

Fig. 8. The wavelet amplitudes of (a) the 850 hPa zonal winds and (b) the SOIs. Contour interval is 0.5 m/sec for the zonal winds and 1 unit for the SOIs, respectively. The area is shaded, where the winds are stronger than 1 m/sec and the values of the index greater than 3 units.

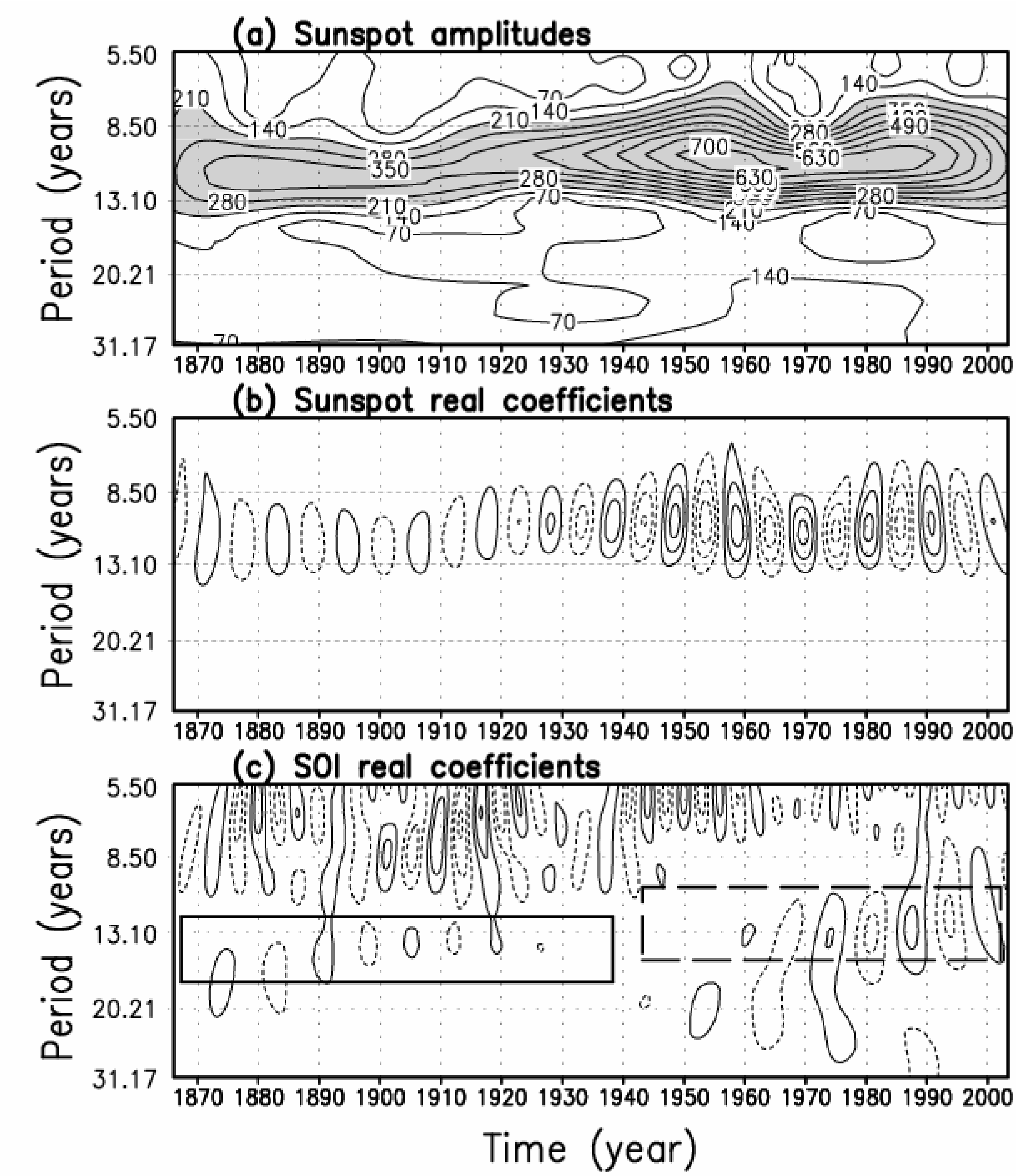

Fig. 9. The (a) amplitudes and (b) real coefficients of the wavelet transform of the sunspot numbers and (c) the real coefficients of the SOI wavelets. The contour interval is 70 and shaded area has sunspot amplitudes larger than 210 in (a). The contour interval in (b) and (c) is 200 and 2, respectively. The solid and dashed rectangles denote the proximate frequency bands in which oscillations may have been induced by the sunspot cycles.

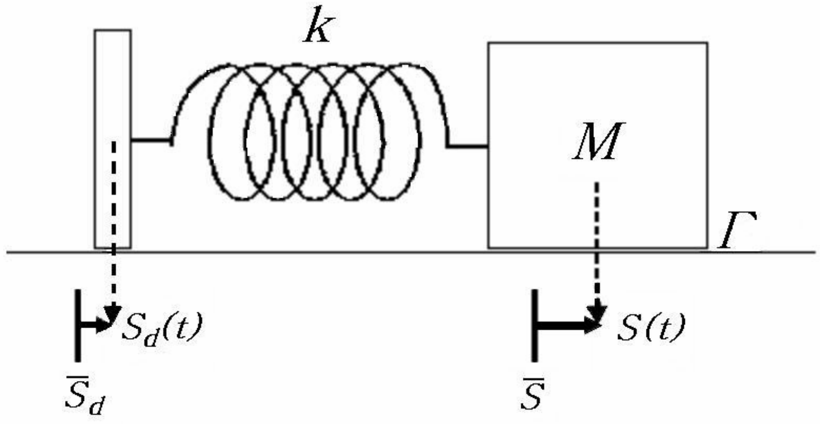

Fig. 10. A schematic diagram for a damped harmonic oscillator in motion $S(t)$ by the forced displacement $S_d(t)$. The system has the natural frequency $\omega_0 = \sqrt{\frac{k}{M}}$, the damped frequency $\omega = \sqrt{\omega_0^2 - (\frac{\Gamma}{2})^2}$, and driving frequency ω_d which can be determined from $S_d(t)$. The symbols are: k a spring constant, M the mass of the moving part, Γ the friction. In our simple manipulation, we assume that the natural periodicity is the same in its length as the sunspot cycle of 10-year period.

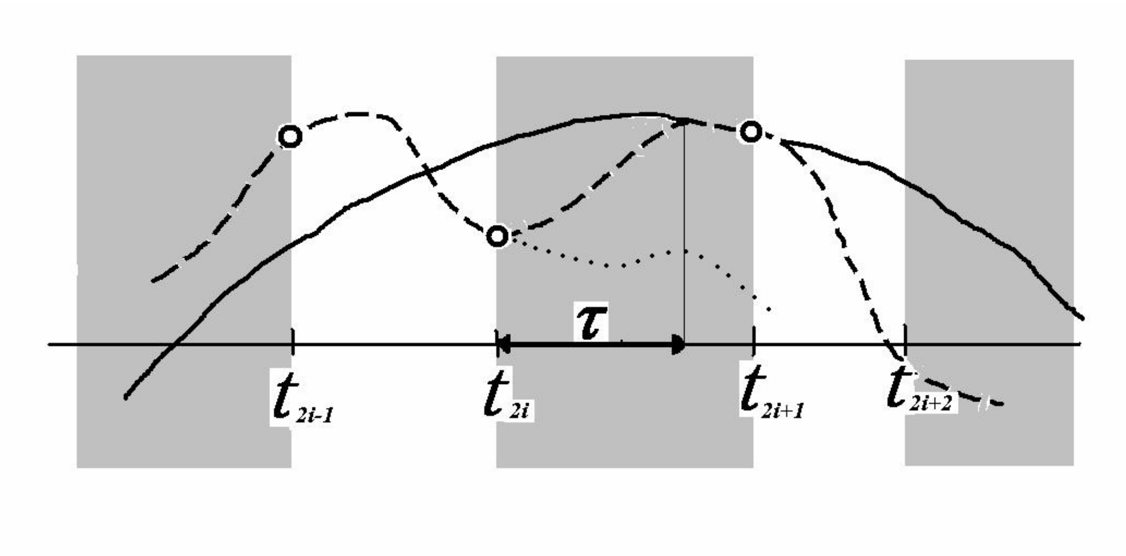

Fig. 11. Piece by peace combination in time of the homogeneous and forced solutions to obtain the composited full solution. The smoothly varying solid curve denotes the forced solution. Time span without shading is dominated by the homogenous solution and shaded time span will have the linear combination of the both solutions for time lapse less than τ and after that forced solution will solely compose the composite solution until the next time step. The subscripted index i denotes time interval from t_{2i} to t_{2i+2} in our expression scheme.

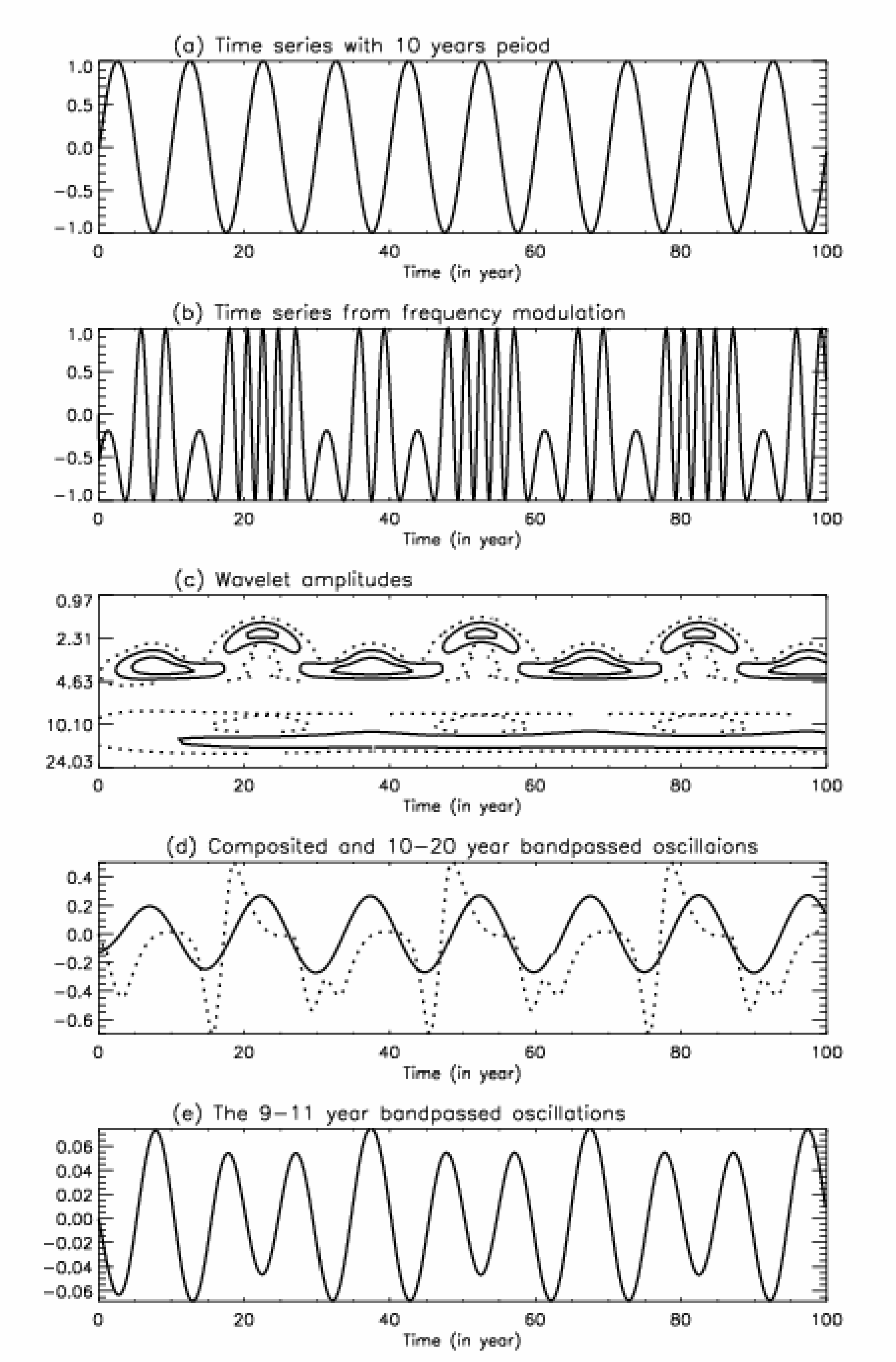

Fig. 12. Simulation of the time series of the 850 hPa zonal winds from a simple harmonic component with 10-period by applying frequency modulation with 30-year period: (a) a sinusoidal wave, (b) frequency modulated time series, (c) the wavelet amplitudes of (b), (d) 15-year period oscillation in a solid line and composite solution in a dotted line, and (d) about 10-year period oscillations. For details, refer to the text.